Bleaching the record: After 200 years, single crystal X-ray crystallography reveals the structure and hydrogen-bonding properties of hypochlorite and hypobromite ions in the solid state

Filip Topić,[a] Joseph M. Marrett,[a] Tristan H. Borchers,[a] Hatem M. Titi,[a] Christopher J. Barrett[a] and Tomislav Friščić[a,*]

[a] Department of Chemistry, McGill University, 801 Sherbrooke St. W., H3A 0B8 Montreal, Canada.

Abstract

We report the first single crystal X-ray structures of hypochlorite and hypobromite salts, including hydrated sodium hypochlorite – a ubiquitous bleaching and disinfection agent in use for almost 200 years. The structures represent the first characterization of fundamentally important hypochlorite and hypobromite anions in the solid state, by X-ray crystallography, and are supported by Raman spectroscopy on individual crystals. The structural analysis provides insight into supramolecular chemistry of the hypohalite ions in the hydrated environment of the $NaOCl{\cdot}5H_2O$ and $NaOBr{\cdot}5H_2O$ solid salts, and reveals measured Cl–O and Br–O bond lengths of 1.69 Å and 1.82 Å, respectively, which are significantly longer than those for corresponding higher-valence oxoanions, and in agreement with the values spectroscopically determined for hypohalous acids and corresponding oxides in the gas phase.

Introduction

The hypochlorite (ClO^-) and hypobromite (BrO^-) are anions of high fundamental importance, ubiquitous in general and main group chemistry textbooks.[1] Hypochlorite is one of the only three

readily isolatable species in which chlorine adopts the rare +1 oxidation state (other two being ClF and Cl_2O),[2] while hypobromite is the heaviest hypohalite species that has so far been isolatable as a solid.[3] Notably, sodium hypochlorite (NaOCl) is a widely used bleaching and sanitizing agent, in use for almost 200 years. The industrial production of hypochlorite bleaching solution (Eau de Javel) was in place in 1788, quickly following Berthellot's report[4,5] on bleaching by aqueous chlorine, and the use of NaOCl as an antiseptic begun in 1820s, following the work of Labarraque.[6] Today, aqueous NaOCl is manufactured on a scale of >2 billion gallons annually (e.g. Clorox®), with a global market estimated at >$260 million boosted by the increased need for sanitizers during the COVID-19 pandemic.[7] It is an ubiquitous chemical with large-scale applications including for water purification, the wood industry, and as a general sanitizer.[8,9] Sodium hypochlorite is commercially available either as a basic aqueous solution, or as a low-melting hydrated solid – reported by Muspratt[10] in 1898 and subsequently established to be a pentahydrate ($NaOCl \cdot 5H_2O$).[11] This readily prepared[12] hydrate has found application as an oxidant in organic synthesis,[13,14] and recently also in mechanochemistry.[15] The BrO^- ion has also found applications as an oxidant, notably in as an *in situ* formed species in the Hofmann rearrangement,[16] and is sometimes used as an alternative to hypochlorite in water sanitization, formed *in situ* from aqueous NaBr solutions.[17] The preparation of a solid sodium hypobromite hydrate ($NaOBr \cdot 5H_2O$) was reported in 1952 by Scholder and Krauss.[18]

Despite the fundamental, historical, and practical significance of hypochlorites and hypobromites, as well as accessibility of crystalline solid forms for at least 120 years in case of ClO^-, and 70 years in case of BrO^-, no crystal structures containing the ClO^- or BrO^- anion appear to have been reported, and most structural characterization was performed in the gas phase on the corresponding acids HOCl and HOBr.[19-22] Targeted searches of the Inorganic Crystal Structure

Database (ICSD) for terms hypochlorite, hypobromite, as well as searches for systems containing chlorine and oxygen did not reveal any hypochlorite or hypobromite structures except a theoretical and experimentally not verified model for $2Ca(OH)_2 \cdot Ca(OCl)_2$. A search of the Cambridge Structural Database (CSD) for all structures containing a O-X unit (where X = any halogen) revealed only one relevant structure, of the complex cation $Br_3O_4^+$ with a terminal O-Br group.[23] Consequently, almost 250 years since the discovery and beginning of the industrial manufacture of bleach, there appear to be no experimental crystal structures of either a hypochlorite or a hypobromite ion. It appears that the OCl^- and OBr^- ions remain the only halogen oxoanions that have been prepared in the solid state, and are extensively discussed in textbooks, but have yet to be experimentally characterized by X-ray crystallography.

Here, we report the detailed structural analysis of $NaOCl \cdot 5H_2O$ and $NaOBr \cdot 5H_2O$ using single crystal X-ray diffraction, providing the first X-ray crystallographic observation of the fundamentally important hypochlorite and hypobromite ions in the solid state, accompanied by variable-temperature Raman spectroscopy of individual crystals.

Results

Sodium hypochlorite pentahydrate ($NaOCl \cdot 5H_2O$)

There have been several attempts to characterize hypochlorites in the solid state. In 1935, Bunn[24] reported the unit cell parameters of dibasic calcium hypochlorite $Ca(OCl)_2 \cdot 2Ca(OH)_2$ through powder X-ray diffraction (PXRD),[13] and in 1968 Aleksandrova and co-workers[25] proposed a model for the structure by replacing one third of all OH groups in the $Ca(OH)_2$ structure by ClO^- units. This structural model, which was not experimentally validated, exhibits an unrealistically long (2.1 Å) Cl-O bond in ClO^-. In 1999, Kiselev *et al.* used PXRD to determine the unit cell

dimensions of $LiOCl{\cdot}H_2O$, and suggested the compound could be structurally similar to α-CeSI.[26] Solid $NaOCl{\cdot}5H_2O$ has been the subject of at least three X-ray single crystal or powder diffraction studies since 1940s,[27-29] which reported different crystallographic unit cells, but without any further structural information (Table 1). The most recent study is reported in patent applications between 2018 and 2020 which used PXRD to establish a tetragonal or orthorhombic unit cell with dimensions a = 16.3(1) Å, b = 5.4(1) Å, and c = 16.2(1) Å.[28,29] Whereas these unit cell parameters are different from those previously reported, we note that they could tentatively be related by doubling the size of one of the crystallographic unit cell edges.

Here, a single crystal of $NaOCl{\cdot}5H_2O$ was obtained from a commercial sample of the material (TCI Chemicals, Lot# 3XN4J-GC). Large (>1 mm in diameter), irregularly shaped crystals of $NaOCl{\cdot}5H_2O$ could be easily distinguished from the smaller cubic crystals of NaCl also present in the sample, but would rapidly liquify at room temperature. However, rapidly transferring a piece of a larger crystal into a cold stream enabled collection of high-resolution X-ray diffraction data and allowed for structure determination.

Table 1. Crystallographic unit cell parameters for the $NaOCl{\cdot}5H_2O$ structure reported here, compared to previously reported unit cell data based on PXRD and single crystal X-ray diffraction.

a / Å	*b* / Å	*c* / Å	Crystal System & Space Group
7.91	15.84	5.28	orthorhombic[a]
8.08	16.06	5.33	orthorhombic[a]
16.3(1)	5.4(1)	16.2(1)	tetragonal or orthorhombic *Pbca*[b,c]
5.3643(2)	16.2061(6)	16.2689(6)	orthorhombic *Pbca*[d,e]
5.3782(1)	16.2899(5)	16.2997(5)	orthorhombic *Pbca*[d,f]

[a]Fehér and Talpay (1944);[27] [a]Fehér, Hirschfeld and Linke (1962);[27] [b]at 123 K; [c]WO2018159233A1[28] and US20200010320;[29] [d]present work; [e]at 173 K; [f]at 253 K.

X-ray diffraction at 173 K and 253 K on the same single crystal of $NaOCl \cdot 5H_2O$ consistently provided an orthorhombic unit cell with parameters resembling those reported in the patent by Okada et al. (Table 1). Notably, whereas the unit cell parameters *b* and *c* at 173 K differ by ca. 0.63 Å (*b*/*c* ratio = 0.9961), the increase in the unit cell parameter *b* at 253 K is approximately three times that for *c*, making the difference less than 0.1 Å (*b*/*c* ratio = 0.9994). The similarity between unit cell parameters *b* and *c* at higher temperatures results in a pseudo-tetragonal unit cell, potentially explaining the conflicting reports of tetragonal and orthorhombic crystal system for $NaOCl \cdot 5H_2O$.

The crystal structure of $NaOCl \cdot 5H_2O$ is composed of alternating tapes of hydrated Na^+ ions, and tapes of ClO^- ions and water molecules (Figure 1a). The tapes are parallel to the crystallographic ac-plane and extend along the crystallographic *a*-direction. The sodium-containing tapes exhibit the composition $[Na(H_2O)_4^+]_n$ and are based on Na^+ ions surrounded by six water molecules in the form of a distorted octahedron, with each cation connected to two neighboring ones through two pairs of bridging water molecules (Figure 1b).

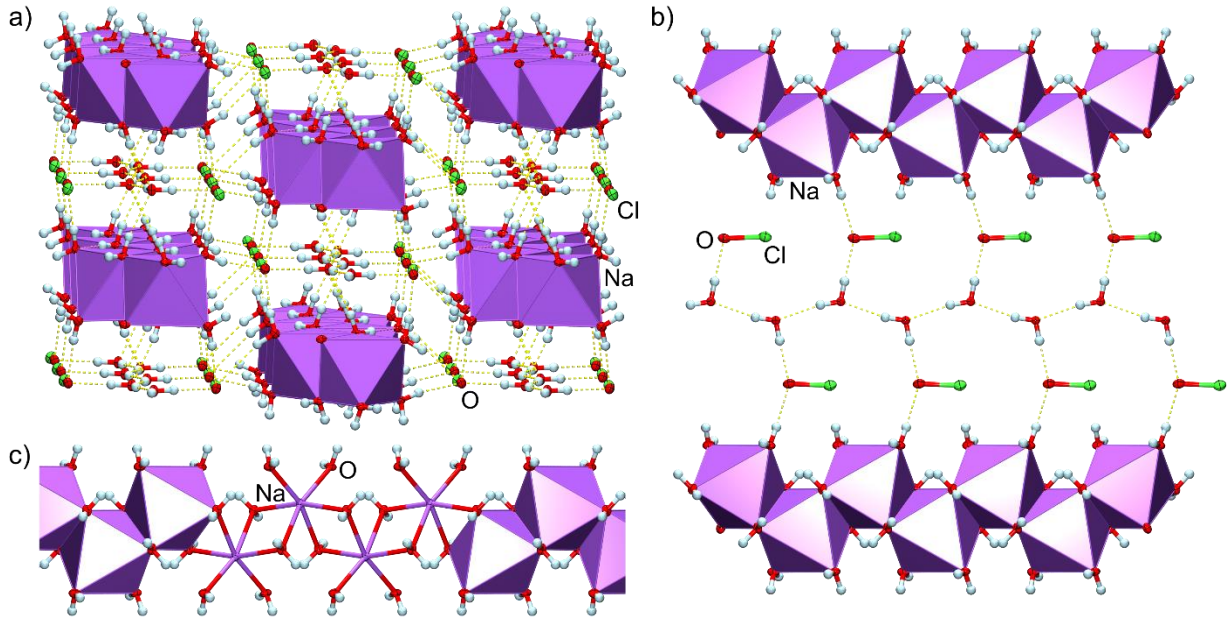

Figure 1. a) Fragment of the crystal structure of $NaOCl \cdot 5H_2O$, viewed parallel to the crystallographic *a*-axis, with chlorine, oxygen and hydrogen atoms shown as spheres, sodium cations shown as polyhedra, and hydrogen bonds as dotted lines; b) a fragment of a single tape of hydrated sodium cations in the structure of $NaOCl \cdot 5H_2O$, with sodium ions in mixed polyhedral and sphere representation to illustrate the overall structure. c) View of the crystal structure of $NaOCl \cdot 5H_2O$ in the crystallographic *ac*-plane, illustrating two tapes of hydrated sodium cations lining a central hypochlorite-containing tape.

The hypochlorite-containing tapes are composed of a central chain of water molecules connected through O–H···O hydrogen bonds (O···O distance 2.792(1) Å at 173 K), running along the crystallographic a-direction and lined by two sets of hydrogen-bonded ClO^- ions (Figure 1c). The ClO^- ions in each tape are aligned in parallel, and do not interact significantly, as evidenced by the shortest Cl···O contact of 3.681(1) Å at 173 K, which is significantly higher that the expected sum of van der Waals radii[30] for the two atoms (3.27 Å). The anions in nearest-neighbor hypochlorite tapes are in a mutually antiparallel orientation, consistent with a centrosymmetric structure. The ClO^- and water molecules in each tape are associated with the surrounding sodium-containing tapes by acting as acceptors of long O–H···O hydrogen bonds (O···O separations in the range of 2.720(1)-2.990(1) Å at 173 K).

The measured Cl-O distance in the ClO^- ion is 1.686(1) Å at 173 K, which is considerably shorter than the 2.1 Å distance in the previously proposed model of the $2Ca(OH)_2 \cdot Ca(OCl)_2$ structure. The current value is consistent with the expected covalent radii of O (0.66 Å) and Cl (1.02 Å) atoms,[19] and with the value of 1.689 Å spectroscopically obtained by Deely for deuterated hypochlorous acid in the gas phase. It is also slightly shorter than the spectroscopically established Cl-O bond length of 1.696(1) Å in Cl_2O gas.[31] The herein observed Cl-O bond length in ClO^- also fits the trend observed for chlorite (≈1.56-1.57 Å),[32] chlorate (≈1.50 Å)[33] and perchlorate (≈1.42-1.43 Å)[34], which are all expected to exhibit a higher bond order than hypochlorite.

Due to challenges in handling $NaOCl \cdot 5H_2O$ at or near room temperature, PXRD analysis of the bulk material was performed by dipping a plastic loop used for mounting single crystals into the polycrystalline bulk sample, and collecting the X-ray diffraction data at different temperatures using a Bruker D8 Venture diffractometer (see Supplementary Information). The data collected at 173 K revealed an excellent match to the PXRD pattern simulated for herein determined structure (Figure 2a, also see Supplementary Information), with additional Bragg reflections appearing upon heating to 283K. The reflections could not be assigned to any of the previously reported crystal structures of potential decomposition products, including NaCl[35], $NaCl \cdot 2H_2O$[36], $NaClO_2 \cdot 3H_2O$[32], $NaClO_3$[33], $NaClO_4$[37], or $NaClO_4 \cdot H_2O$[34].

Sodium hypobromite pentahydrate ($NaOBr \cdot 5H_2O$)

To the best of our knowledge, there have not yet been any reported attempts to elucidate a crystal structure of a hypobromite salt. Hypobromites are generally less stable than corresponding hypochlorite salts, and are not commecially available chemicals. Samples of $NaOBr \cdot 5H_2O$ were prepared following a procedure (see Supplementary Information) similar to that previously reported by Scholder and Krauss,[18] and by Levason *et al.*,[38] through addition of Br_2 liquid to

aqueous NaOH solution kept at –5 °C. Following several hours in a freezer at –20 °C, the yellow-coloured solution affords plate-like yellow crystals that were identified as $NaOBr \cdot 5H_2O$ using single crystal X-ray diffraction and Raman spectroscopy on a single crystal (see Supplementary Information). Crystal structure determination revealed a monoclinic unit cell, space group $P2_1/n$ (Table 2). As $NaOBr \cdot 5H_2O$ readily liquified upon standing in air at or near room temperature, PXRD analysis of the bulk $NaOBr \cdot 5H_2O$ was performed in the same way as for the hypochlorite analogue (see Supplementary Information), by dipping a plastic loop into the polycrystalline bulk sample, and collecting the X-ray diffraction data using the Bruker D8 Venture diffractometer. The PXRD pattern obtained at 173 K represents an excellent match to the one simulated for the herein determined structure of $NaOBr \cdot 5H_2O$, confirming that the structure is representative of the overall sample (Figure 2a). Heating up to 263 K led to appearance of new PXRD signals, some of which were tentatively ascribed to NaBr[39] and $NaBr \cdot 2H_2O$[40] (see Supplementary Information).

Table 2. Crystallographic unit cell parameters for $NaOBr \cdot 5H_2O$ at 173 K and 223 K.

a / Å	b / Å	c / Å	β / °	T / K
9.5985(8)	5.3509(4)	14.1110(11)	95.218(3)	173
9.6131(2)	5.3607(1)	14.1312(4)	95.1215(9)	223

Despite the difference in crystallographic parameters and overall symmetry (Table 2), the crystal structure of $NaOBr \cdot 5H_2O$ is very similar to that of $NaOCl \cdot 5H_2O$ (Figure 2b). In particular, the structure consists of tapes of hydrated sodium cations analogous in structure and composition to those seen in $NaOCl \cdot 5H_2O$, and surrounded by parallel hypobromite-containing tapes composed of a central chain of hydrogen-bonded water molecules (O···O distance 2.792(4) Å) lined on two sides by BrO^- ions (Figure 2c). Just like in the analogous hypochlorite salt, the oxygen atoms of

BrO^- and water molecules in the hypobromite-containing tapes are involved as acceptors in O–H···O hydrogen bonds with water molecules from neighboring tapes of hydrated sodium cations (O···O distances from 2.723(4) to 3.041(4) Å). The most significant difference in the crystal structures of hydrated sodium hypochlorite and hypobromite is a shift in stacking of alternating cation- and anion-containing tapes, reflecting the change from orthorhombic to monoclinic symmetry.

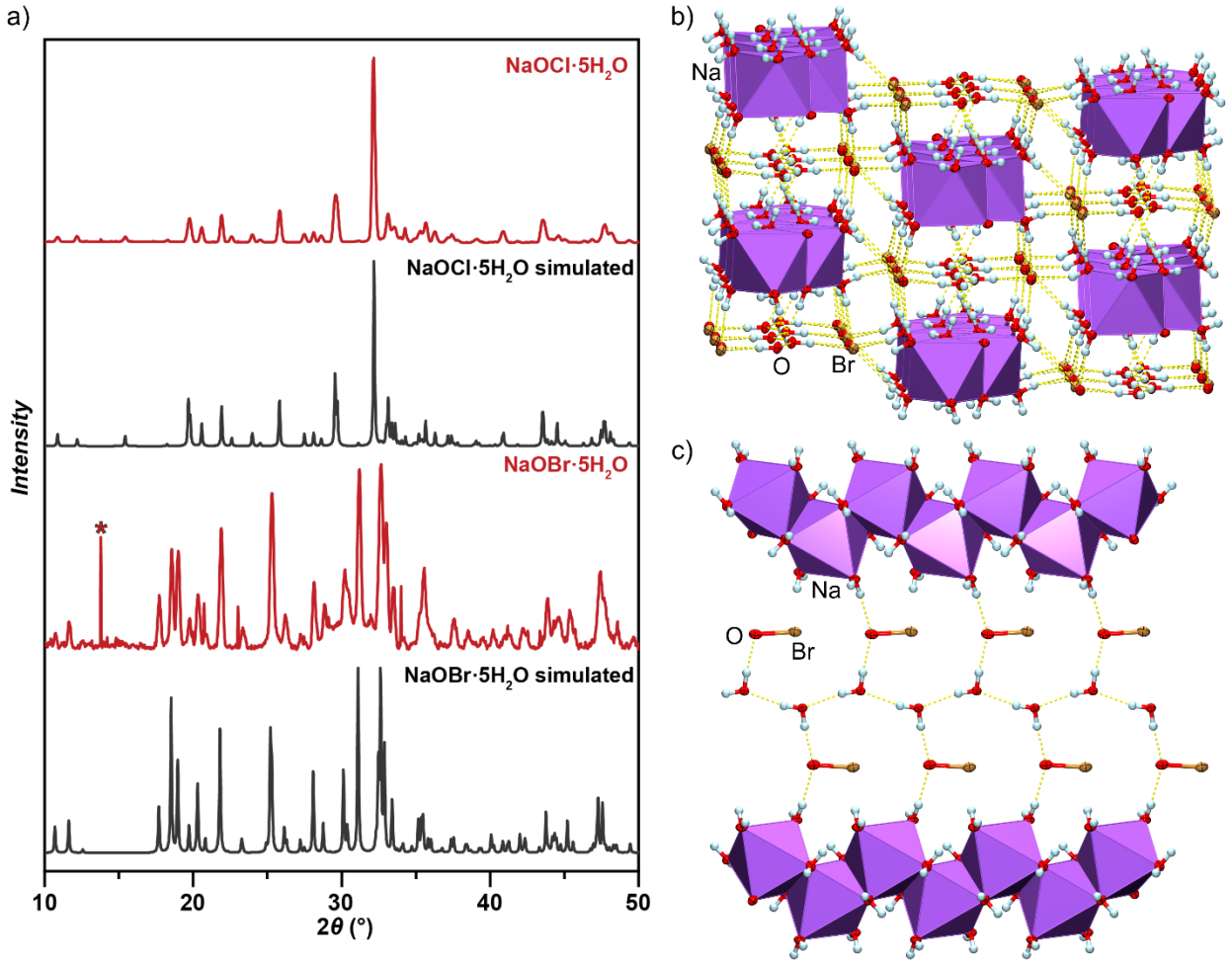

Figure 2. a) Comparison of PXRD patterns simulated for herein determined structures of $NaOCl·5H_2O$ and $NaOBr·5H_2O$ with the ones measured at 173 K for bulk microcrystalline samples. The measured patterns also contain narrow reflections coming from the sample holder, one of which is highlighted by a '*'. Different views of the crystal structure of $NaOBr·5H_2O$: c) along the crystallographic b-axis and parallel to tapes of hydrated Na^+ ions (shown in polyhedral representation) and hydrogen-bonded BrO^- ions (shown as ellipsoids); c) perpendicular to a hydrogen-bonded tape of hypobromite ions.

The measured Br-O distance in the BrO^- ion is 1.820(3) Å at 173 K (1.824(2) Å at 223 K). This value is significantly shorter than the Br-O bond length of the terminal OBr unit of the cation $Br_3O_4^+$ (≈1.93 Å) reported by Seppelt,[23] but is in close agreement with the gas-phase spectroscopic Br-O bond length estimates of 1.828 Å and 1.834 Å for hypobromous acid.[20,21] The herein measured length of the Br-O bond in the hypobromite anion is also slightly shorter than the vale spectroscopically established for Br_2O in the gas phase (1.85 Å).[41] It is also notably longer than observed in other oxoanions of bromine in the solid state (≈1.70-1.73 Å in $NaBrO_2 \cdot 3H_2O$,[42] ≈1.65 Å in $NaBrO_3$,[33] and ≈1.60 Å in $NaBrO_4 \cdot H_2O$[43]), fitting the expected overall trend of bond length shortening with an increase in the oxidation state of the halogen atom.

Theoretical modelling

The experimentally established overall structures of $NaOCl \cdot 5H_2O$, $NaOBr \cdot 5H_2O$, and the structures of the underlying hydrogen-bonded frameworks have been verified by energy minimization using periodic density functional theory (DFT) through the plane-wave code CASTEP.[44] Besides validating the herein determined crystal structures, we were also curious to see how well the different functionals and the use of semi-empirical dispersion correction (SEDC) can reproduce the experimentally determined crystallographic data. For this purpose, we conducted the optimization using either the Perdew-Burke-Ernzerhof (PBE)[45] and LDA[46] functionals, and also using the PBE functional combined with the recently popular Grimme's D2,[47] D3,[48] D3(BJ)[49] and Tkatchenko-Scheffler TS[50] semi-empirical dispersion approaches. In all cases, the energy optimization yielded very little change to the structure (Figure 3, also see Supplementary Information), with most employed functionals and SEDC strategies yielding no more than 5% difference between the experimentally obtained unit cell dimensions and those

following DFT optimization. While optimization using the LDA functional led to 4-6% underestimation of each unit cell parameter and a 14% underestimation of the unit cell volume, a better match was obtained using the PBE functional, illustrated by a ca. 4.5% (for $NaOCl \cdot 5H_2O$) and 4.2% (for $NaOBr \cdot 5H_2O$) difference between calculated and measured cell volumes. Significantly improved results were obtained by optimization using the PBE approach in combination with different SEDC strategies. A particularly good match of the optimized unit cell parameters to the experimental data (no more than 0.89% for $NaOCl \cdot 5H_2O$ and 1.36% for $NaOBr \cdot 5H_2O$), accompanied by only a ca. 2% change in unit cell volume, was obtained using PBE+TS, indicating this approach as well-suited for modelling the herein reported salts. Most importantly, in all cases there was no change in the overall connectivity of the hydrogen-bonded framework, confirming the validity of the X-ray single crystal structure determination.

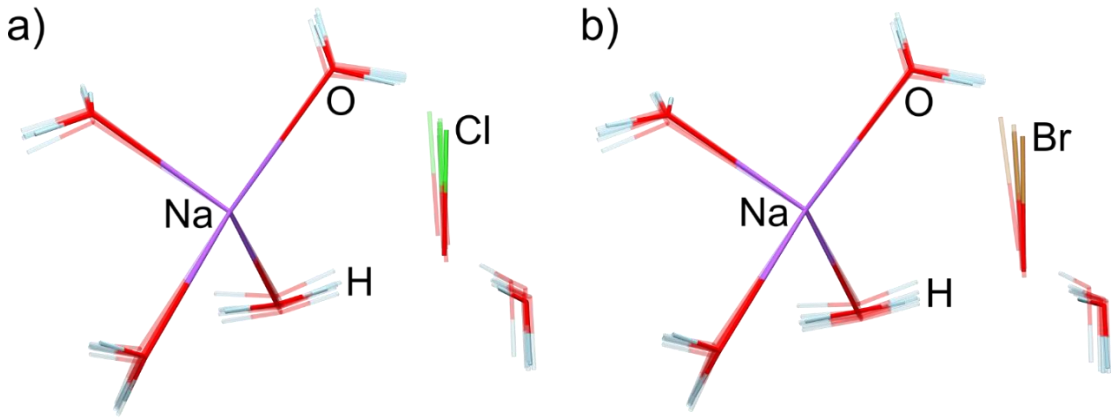

Figure 3. Overlay of the contents of the asymmetric unit for crystal structures after DFT optimization: a) $NaOCl \cdot 5H_2O$ and b) $NaOBr \cdot 5H_2O$. The methods used for optimization were based on the PBE and LDA functionals, as well as the PBE functional combined with D2, D3, D3(BJ) and TS SEDC approaches. Details of calculations and differences between structures optimized using different methods are given in the Supplementary Information.

Hydrogen bonding behaviour of OCl^- and OBr^-

The crystal structures of sodium hypochlorite and hypobromite provide a unique opportunity to explore the interactions of ClO^- and BrO^- ions, respectively, with surrounding

molecules of water. Notably, the structures reveal significant differences in hydrogen bonding behaviour between the oxygen and the halogen atoms in each hypohalite salt. The oxygen atom of each ClO^- ion is anchored as an acceptor of four short charge-assisted[51] O–H···O hydrogen bonds (Figure 4a), three of which are longer (O···O separations 2.720(1) Å, 2.743(1) Å, and 2.854(1) Å at 173 K) and come from water molecules in three surrounding sodium-containing tapes. The fourth and shortest O–H···O hydrogen bond (O···O separation of 2.665(1) Å at 173 K) to the hypochlorite ion comes not from a water molecule associated with a Na^+ cation, but from one that belongs to the central hydrogen-bonded chain of the belonging hypochlorite-containing tape. This is perhaps counter-intuitive, as the shortest hydrogen bond to an anion would be expected to form through water molecules attached to a cation.

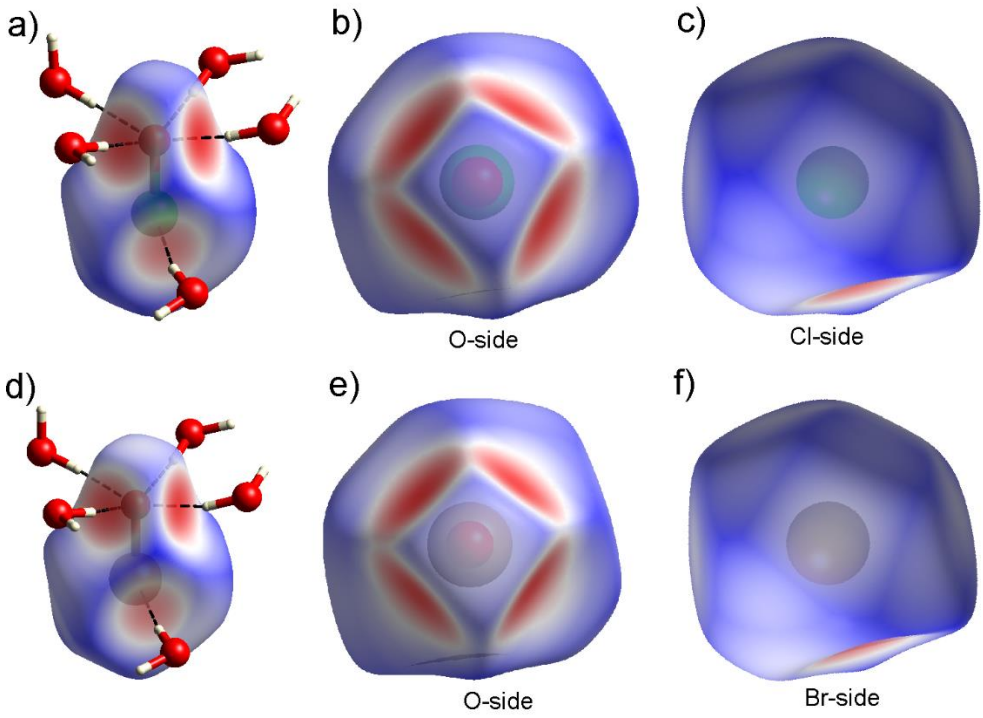

Figure 4. Hirshfeld surfaces illustrating close interactions to hypohalite anions in $NaOCl·5H_2O$ and $NaOBr·5H_2O$. Views of the hypochlorite ion: a) illustrating the presence of four O-H···O hydrogen bonds and a O-H···Cl contact; b) illustrating the environment of the oxygen and c) illustrating the environment of the chlorine atom. Views of the hypobromite ion: d) illustrating the presence of four O-H···O hydrogen bonds and a O-H···Cl contact; e) illustrating the environment of the oxygen and f) illustrating the environment of the chlorine atom.

In contrast, the chlorine atom of the hypochlorite does not appear to participate in any significant interactions except a long O−H···Cl hydrogen bonding contact (Figure 4a) coming from a neighboring sodium-containing tape. The O···Cl distance for this contact at 173 K is 3.275(1) Å, which is right at the limit of the sum of the van der Waals radii for Cl (1.75 Å) and O (1.52 Å), while the corresponding H···Cl separation is 2.45 Å, which is ~0.4 Å or 15% shorter than the sum of van der Waals radii of H and Cl 2.85 Å). At 253 K, the O···Cl distance is 3.2883(7) Å, comfortably above the sum of the van der Waals radii, and the H···Cl separation is 2.46 Å, overall indicating a weak hydrogen bond. Consequently, in terms of hydrogen bonding behaviour, the chlorine atom of the hypochlorite ion appears to be similar to covalently-bound chlorine in organic molecules, which does not readily form hydrogen bonds with strong O−H donors.[52] The difference in supramolecular chemistry between oxygen and chlorine atoms of the hypochlorite ion is evident from the Hirshfeld surface analysis,[53] revealing a polyhedral shape influenced by short contacts for the oxygen atom, and a more isometric shape for the chlorine atom (Figure 4b,c).

Similar hydrogen-bonding behaviour is observed in the structure of $NaOBr·5H_2O$, where each hypobromite ion is involved as an acceptor in four O−H···O hydrogen bonds (Figure 4d). Similar to the structure of $NaOCl·5H_2O$, three of these hydrogen bonds are longer and form with water molecules from three different tapes of hydrated sodium ions (O···O separations: 2.723(4) Å, 2.777(4) Å, and 2.847(3) Å at 223 K), while one is shorter (O···O separation of 2.670(4) Å) and established with a water molecule from the central hydrogen-bonded chain of the corresponding anion-containing tape. The bromine atom of the BrO^- ion does not participate in any significant intermolecular interactions, except a long O−H···Br contact to a neighbouring water molecule (Figure 4d). The corresponding O···Br distance is 3.389(3) Å at 173 K (3.395(2)

Å at 223K), which is slightly longer that the expected sum of van der Waals radii for bromine and oxygen (3.35 Å) and indicates a potentially very weak hydrogen bond. In the case of BrO^- also, the difference in hydrogen bonding properties between the oxygen and halogen atoms is clearly evident in comparison of Hirshfeld plots (Figure 4e,f).

Raman spectroscopy and optical microscopy

The presence of hypohalite ions in single crystals of both $NaOCl{\cdot}5H_2O$ and $NaOBr{\cdot}5H_2O$ was also confirmed by Raman spectroscopy on individual crystals. In particular, Raman spectra of several crystals of commercial $NaOCl{\cdot}5H_2O$ revealed a strong band at 711 cm^{-1}, which is consistent with the previously reported ν(Cl-O) stretching band at 713 cm^{-1} for aqueous NaOCl (Figure 5a).[54] Similarly, Raman spectroscopy of a single crystal of $NaOBr{\cdot}5H_2O$ confirmed the presence of the OBr^- ion through a band at 622 cm^{-1}, which is consistent with value of 620 cm^{-1} that were previously reported for the hypobromite ν(Br-O) stretching in solution (Figure 5b).[38,55] Observation of single crystals of $NaOCl{\cdot}5H_2O$ and $NaOBr{\cdot}5H_2O$ using simultaneous Raman spectroscopy and optical microscopy allowed an exploration into characterization of their thermal behaviour.

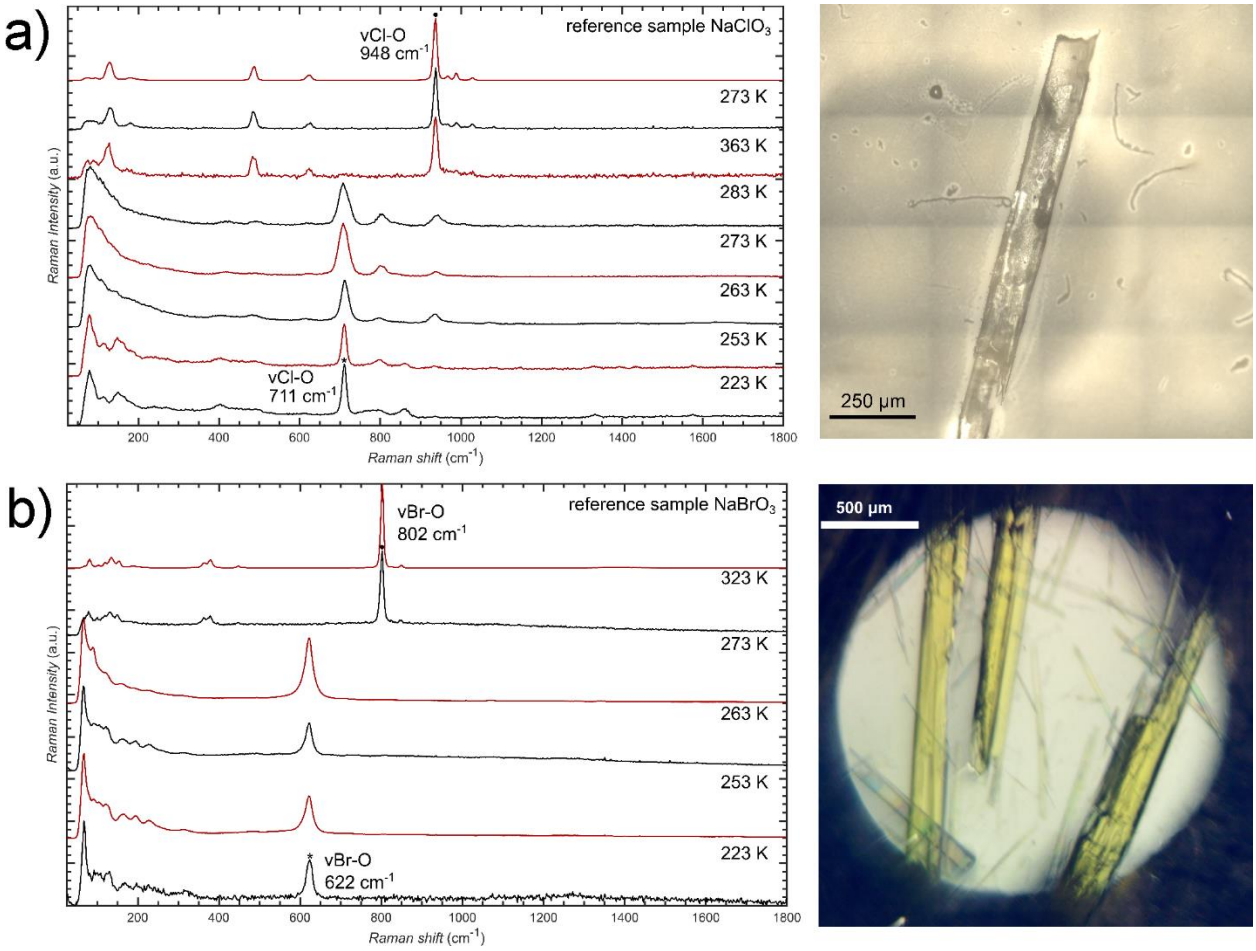

Figure 5. Raman spectroscopy and optical microscopy images of $NaOCl{\cdot}5H_2O$ and $NaOBr{\cdot}5H_2O$. a) left: Raman spectra of a sample of $NaOCl{\cdot}5H_2O$ taken at different temperatures, compared reference sample of $NaClO_3$ and right: optical microscopy image of a representative crystal of $NaOCl{\cdot}5H_2O$. b) left: Raman spectra of a sample of $NaOBr{\cdot}5H_2O$ taken at different temperatures, compared to reference sample of $NaBrO_3$ and right: optical microscopy image of a representative sample of $NaOBr{\cdot}5H_2O$.

Heating of the hypohalite salts leads to the broadening of their fundamental $X\text{-}O^-$ (X = Cl, Br) Raman band and disappearance of low frequency bands (< 200 cm^{-1}), consistent with the transformation to form a liquid phase that is also observed by optical microscopy. In particular, heating of $NaOCl{\cdot}5H_2O$ crystals up to ca. 20 °C leads to the formation of a liquid phase, followed upon further heating by the disappearance of the 711 cm^{-1} Raman signal and concomitant appearance of a new set of Raman bands: a strong one at 948 cm^{-1} and a weaker one at 684 cm^{-1}.

These new bands are entirely consistent with the separately measured spectrum of sodium chlorate ($NaClO_3$), which aligns with the expected thermal disproportionation of hypochlorite into chloride and chlorate (Figure 5a, also see Supplementary Information).

Samples of $NaOBr \cdot 5H_2O$ crystals were found to liquify across a temperature range from 0 to 22 °C (see Supplementary Information). We explain the absence of a sharp melting point through crystal dissolution in small amounts of residual mother liquour. Further heating of $NaOBr \cdot 5H_2O$ shows a recrystallization occurring at 50 °C, along with the change in sample colour from yellow to colourless. Raman spectroscopy monitoring during sample heating reveals the disappearance of the band at 622 cm^{-1} and concomitant appearance of a new Raman signal at 802 cm^{-1}. The resulting Raman spectrum is entirely consistent with a separately measured one for a sample of sodium bromate ($NaBrO_3$, Figure 5b). The described changes in the Raman spectrum and sample appearance are consistent with the expected thermal disproportionation of hypobromite into BrO^- and Br^-. Indeed, X-ray structure characterization for a crystal resulting from a hypobromite reaction mixture that was not adequately cooled revealed a previously unreported mixed hydrated salt of composition $Na_3(BrO_3)_2Br \cdot 2H_2O$. Single crystal X-ray structure analysis (see Supplementary Information) of this salt revealed two types of sodium ions based on the coordination environment. One type of Na^+ ions is characterized by a distorted square antiprismatic environment, formed by eight oxygen atoms of four bromate ions, where each BrO_3^- acts as a bidentate ligand (Na···O distances 2.430(2) Å – 2.734(2) Å). The second type of Na^+ ions are surrounded by a bromide (Na···Br distance 3.167(1) Å) ion and five oxygen atoms (Na···O distances 2.370(2) Å – 2.417(2) Å), coming from three bromate ions and two molecules of water, in the shape of a distorted octahedron. The octahedra are connected through the Br^- and oxygen atoms of water molecules acting as μ_2-bridging ligands. The structure and composition of this

mixed anion salt are consistent with the expected disproportionation of hypobromite to a mixture of bromide and bromate.[1-3,56]

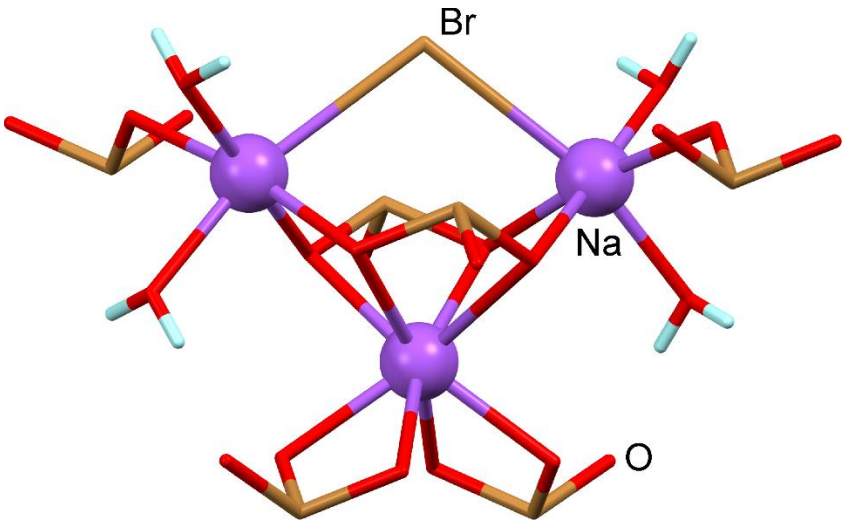

Figure 6. Fragment of the crystal structure of $Na_3(BrO_3)_2Br{\cdot}2H_2O$, illustrating bromide-bridged sodium cations with distorted octahedral coordination, and sodium cations surrounded by four BrO_3^- ions in a distorted square antiprism environment. The structure view is close to parallel with the crystallographic *c*-axis.

Conclusions

In summary, we have provided the first single crystal X-ray diffraction structural characterization of solid hypochlorite and hypobromite salts. The herein determined and described structures represent long-missing contributions to the understanding of fundamental chemistry of halogens, and in particular to sodium hypochlorite: the active component of liquid bleach and a chemical that has been the staple of chlorine industry for almost two centuries. Besides providing the so-far first reports of the geometry of ClO^- and BrO^- ions in the solid state, we also find that the water-rich environment in the structures of the solid $NaOCl{\cdot}5H_2O$ and $NaOBr{\cdot}5H_2O$ salts provides a unique opportunity to investigate the supramolecular hydrogen-bonding behaviour of the hypohalite ions. In particular, the herein determined structures indicate that the covalently bound

chlorine and bromine atoms of the hypohalite ions do not participate in strong hydrogen bonding, in that way resembling halogens in halogenated organic molecules.

Acknowledgments

We thank Dr. Dejan-Krešimir Bučar (University College London), Assoc. Prof. Dominik Cinčić (University of Zagreb), and Dr. Andrew J. Morris (University of Birmingham) for valuable discussions and literature overviews.

References

1 L. Pauling, General Chemistry. Dover Publications, Inc. New York (1988).

2 J.-P. Liang, Chlorine, Bromine, Iodine & Astatine: Inorganic Chemistry. In: Encyclopedia of Inorganic and Bioinorganic Chemistry, Online, Wiley (2011).

3 R. B. King, Inorganic Chemistry of Main Group Elements. Wiley-VCH (1994).

4 C. L. Berthollet, Description du Blanchiment des Toiles et des Fils par l'Acide Muriatique Oxygéné, et de Quelques Autres Propriétés de Cette Liqueur Relatives Aux Arts, *Annales de Chimie*, 1789, *2*, 151-190.

5 P. Dorveaux, L'invention de l'eau de Javel. *Revue d'Histoire de la Pharmacie*, 1929, 63, 286–287.

6 J. Scott, On the Disinfecting Properties of Labarraque's Preparations of Chlorine. 3rd Edition, Published by S. Highley, 174 Fleet Street, London (1828).

7 https://www.fortunebusinessinsights.com/sodium-hypochlorite-market-105064

8 H. Vogt, J. Balej, J. E. Bennett, P. Wintzer, S. A. Sheikh, P. Gallone, S. Vasudevan, K. Pelin, Chlorine Oxides and Chlorine Oxygen Acids. *Ullmann's Encyclopedia of Industrial Chemistry, Vol. 8*, 2010, 624-684.

9 T. F. O'Brien, T. V. Bomaraju, F. Hine, Handbook of Chlor-Alkali Technology, Vol. 1: Fundamentals. Springer Science+ Business Media, Inc. (2008).

10 M. Muspratt, S. Smith, Some Experiments upon High Strength Hypochlorite Solutions. *Journal of the Society of Chemical Industry*, 1898, *17*, 1096-1100.

11 M. P. Applebey, Sodium Hypochlorite. *J. Chem. Soc., Trans.* 1919, 115, 1106-1109.

12 G. Brauer, Handbook of Preparative Inorganic Chemistry, Vol. 1. Academic Press, New York (1963).

13 M. Kirihara, T. Okada, Y. Sugiyama, M. Akiyoshi, T. Matsunaga, Y. Kimura, Sodium Hypochlorite Pentahydrate Crystals ($NaOCl \cdot 5H_2O$): A Convenient and Environmentally Benign Oxidant for Organic Synthesis. *Org. Process Res. Dev.* 2017, 21, 1925-1937.

14 R. V. Stevens, K. T. Chapman, Further Studies on the Utility of Sodium Hypochlorite in Organic Synthesis. Selective Oxidation of Diols and Direct Conversion of Aldehydes to Esters. *Tet. Letters.* 1982, 23, 4647-4650.

15 A. Porcheddu, F. Delogu, L. De Luca, C. Fattuoni, E. Colacino. Metal-free mechanochemical oxidations in Ertalyte® jars. *Beil. J. Org. Chem.* 2019, 15, 1786-1794.

16 Z. Wang, Comprehensive Organic Name Reactions and Reagents. John Wiley & Sons (2010), 1447-1450.

17 Alternative drinking-water disinfectants: bromine, iodine and silver. World Health Organization, Geneva, 2018.

18 R. Scholder, K. Krauss, Über kristallisierte Alkalihypobromite. *Zeit. Anorg. Allg. Chem.* 1952, 268, 279-290.

19 C. M. Deeley, Vibration-Rotation Spectra of Deuterated Hypochlorous Acid and the Determination of the Equilibrium Structure. *J. Mol. Spectr.* 1987, 122, 481-489.

20 Y. Koga, H. Takeo, S. Kondo, M. Sugie, C. Matsamura, The Rotational Spectra, Molecular Structure, Dipole Moment, and Hyperfine Constants of HOBr and DOBr. *J. Mol. Spectr.* 1989, 138, 467-481.

21 E. A. Cohen, G. A. McRae, T. L. Tan, R. R. Friedl, J. W. C. Johns, M. Noël, The ν_1 Band of HOBr. *J. Mol. Spectr.* 1995, 173, 55-61.

22 R. M. Escribano, G. Di Lonardo, L. Fusina, Empirical Anharmonic Force Field and Equilibrium Structure of Hypochlorous Acid, HOCl. *Chem. Phys. Lett.* 1996, 259, 614-618.

23 K. Seppelt, Reactions of Bromine Fluoride Dioxide, BrO_2F, for the Generation of the Mixed-Valent Bromine Oxygen Cations $Br_3O_4^+$ and $Br_3O_6^+$. *Angew. Chem. Int. Ed.* 2019, 58, 18928-18930.

24 C. W. Bunn, L. M. Clark, I. L. Clifford, The Constitution and Formation of Bleaching Powder. *Proc. Roy. Soc. A*, 1935, 151, 141-167.

25 M. M. Aleksandrova, G. A. Dmitriev, R. L. Avojan, The probable model of the crystal structure of the two-base calcium hypochlorite (in Russian). *Armen. Khim. Zhur.* 1968, 21, 380-386.

26 Yu. M. Kiselev, L. S. Skogareva, L. N. Kholodovskaya, On the Structures of Hypochlorites: Lithium Hypochlorite Monohydrate. *Russ. J. Inorg. Chem.* 1999, 44, 869-871.

27 F. Fehér, D. Hirschfeld, K.-H. Linke, Zur Kristallstruktur des Natriumhypochlorits, $NaClO{\cdot}5H_2O$. *Acta Cryst.* 1962, 15, 1188-1189.

28 T. Okada, H. Shimazu, H. Ito, Y. Sugiyama, T. Toyama, K. Shimada, H. Fujihisa, S. Takeya, T. Matsunaga, Y. Gotoh, Crystalline Form of Sodium Hypochlorite Pentahydrate and Method for Producing Same. WO/2018/159233 (2018).

29 T. Okada, H. Shimazu, H. Ito, Y. Sugiyama, T. Toyama, K. Shimada, H. Fujihisa, S. Takeya, T. Matsunaga, Y. Gotoh, Sodium Hypochlorite Pentahydrate Crystals and Method for Producing Same. US20200010320 (2020).

30 M. Mantina, A. C. Chamberlin, R. Valero, C. J. Cramer, D. G. Truhlar, Consistent van der Waals Radii for the Whole Main Group. *J. Phys. Chem. A* 2009, 113, 5806-5812.

31 M. Sugie, M. Ayabe, H. Takeo, C. Matsamura, Microwave spectra of dichlorine monoxide in its excited vibrational states. *J. Mol. Struc.* 1995, *352-353*, 259-265.

32 V. Tazzoli, V. Riganti, G. Giuseppetti, A. Coda, The Crystal Structure of Sodium Chlorite Trihydrate, $NaClO_2 \cdot 3H_2O$. *Acta Cryst.* 1975, *B31*, 1032-1037.

33 S. C. Abrahams, J. L. Bernstein, Remeasurement of Optically Active $NaClO_3$ and $NaBrO_3$. *Acta Cryst.* 1977, *B33*, 3601-3604.

34 B. Berglund, J. O. Thomas, R. Tellgren, Hydrogen Bond Studies. CII.* An X-ray Determination of the Crystal Structure of Sodium Perchlorate Monohydrate, $NaClO_4.H_2O$. *Acta Cryst.* 1975, B31, 1842-1846.

35 R. W. Wyckoff, *Crystal Structures*. (Interscience Publishers, 1963).

36 A. A. C. Bode, P. G. M. Pulles, M. Lutz, W. J. M. Poulisse, S. Jiang, J. A. M. Meijer, W. J. P. van Enckevort, E. Vlieg, Sodium Chloride Dihydrate Crystals: Morphology, Nucleation, Growth, and Inhibition. *Cryst. Growth Des.* 2015, 15, 3166-3174.

37 W. H. Zachariasen, The Crystal Structure of Sodium Perchlorate, $NaClO_4$. *Z. Kristallogr. Mineral. Petrogr,* 1930, 73, 141.

38 W. Levason, J. S. Ogden, M. D. Spicer, N. A. Young, Characterisation of the Oxo-anions of Bromine BrO_x^- (x = 1—4) by Infrared, Raman, Nuclear Magnetic Resonance, and Bromine K-Edge Extended X-Ray Absorption Fine Structure Techniques. *J. Chem. Soc. Dalton Trans.* 1990, 349-353.

39 H. Ott, Die Strukturen von MnO, MnS, AgF, NiS, SnJ_4, $SrCl_2$, BaF_2; Präzisionsmessungen einiger Alkalihalogenide. *Z. Kristallogr. Mineral. Petrogr*, 1926, 73, 222.

40 W. R. Haaf, The Crystal Structure of Sodium Bromide Dihydrate. *Acta Cryst.* 1964, 17, 730-732.

41 W. Levason, J. S. Ogden, M. D. Spicer, N. A. Young. Characterization of Dibromine Monoxide (Br_2O) by Bromine K-Edge EXAFS and IR Spectroscopy. *J. Am. Chem. Soc.* 1990, *112*, 1019-1022.

42 W. Levason, J. S. Ogden, M. D. Spicer, M. Webster, N. A. Young. Characterization of Sodium Bromite by X-ray Crystallography and Bromine K-Edge EXAFS, IR, Raman, and NMR Spectroscopies. *J. Am. Chem. Soc.* 1989, *111*, 6210-6212.

43 A. C. Blackburn, J. C. Gallucci, R. E. Gerkin, W. J. Reppart. Structure of Sodium Perbromate Monohydrate. *Acta Cryst.* 1992, *C48*, 419-424.

44 S. J. Clark, et al. First principles methods using CASTEP. *Z. Kristallogr*. 2005, 220, 567–570.

45 J. P. Perdew, K. Burke, M. Ernzerhof, Generalized Gradient Approximation Made Simple. *Phys. Rev. Lett.* 1996, 77, 3865–3868.

46 W. Kohn, L. J. Sham, Self-Consistent Equations Including Exchange and Correlation Effects. *Phys. Rev.* 1965, 140, A1133–A1138.

47 S. Grimme, Semiempirical GGA-type density functional constructed with a long-range dispersion correction. *J. Comp. Chem.* 2006, 27, 1787–1799.

48 S. Grimme, J. Antony, S. Ehrlich, H. Krieg, A consistent and accurate *ab initio* parametrization of density functional dispersion correction (DFT-D) for the 94 elements H-Pu. *J. Chem. Phys.* 2010, 132, 154104.

49 S. Grimme, S. Ehrlich, L. Goerigk, Effect of the damping function in dispersion corrected density functional theory. *J. Comp. Chem.* 2011, 32, 1456–1465.

50 A. Tkatchenko, M. Scheffler, Accurate Molecular Van Der Waals Interactions from Ground-State Electron Density and Free-Atom Reference Data. *Phys. Rev. Lett.* 2009, 102, 073005.

51 P. Gilli, V. Bertolasi, V. Ferretti, G. Gilli, Covalent Nature of the Strong Homonuclear Hydrogen Bond. Study of the O—H---O System by Crystal Structure Correlation Methods. *J. Am. Chem. Soc.* 1994, *116*, 909-915.

52 R. Banerjee, G. R. Desiraju, R. Mondal, J. A. K. Howard, Organic Chlorine as a Hydrogen-Bridge Acceptor: Evidence for the Existence of Intramolecular O—H···Cl—C Interactions in Some *gem*-Alkynols. *Chem. Eur. J.* 2004, *10*, 3373-3383.

53 M. A. Spackman, D. Jayatilaka, Hirshfeld surface analysis. *CrystEngComm* 2009, *11*, 19-32.

54 Z. Wu, A. Wang, Z. Ling, Spectroscopic Study of Perchlorates and Other Oxygen Chlorides in a Martian Environmental Chamber. *Earth Plan. Sci. Lett.* 2016, *452*, 123-132.

55 J. C. Evans, G. Y-S. Lo, Vibrational spectra of BrO^-, BrO_2^-, Br_3^-, and Br_5^-. *Inorg. Chem.* 1967, 6,1483-1486.

56 M. H. Hashmi, A. A. Ayaz, A. Rashid, E. Ali, Stability of Hypobromite and Hypoiodite Reagents. *Anal. Chem.* 1964, 36, 1379-1382.